ICARUS' INDIVIDUALS

AME 105 Glider Report

December 1st, 2022

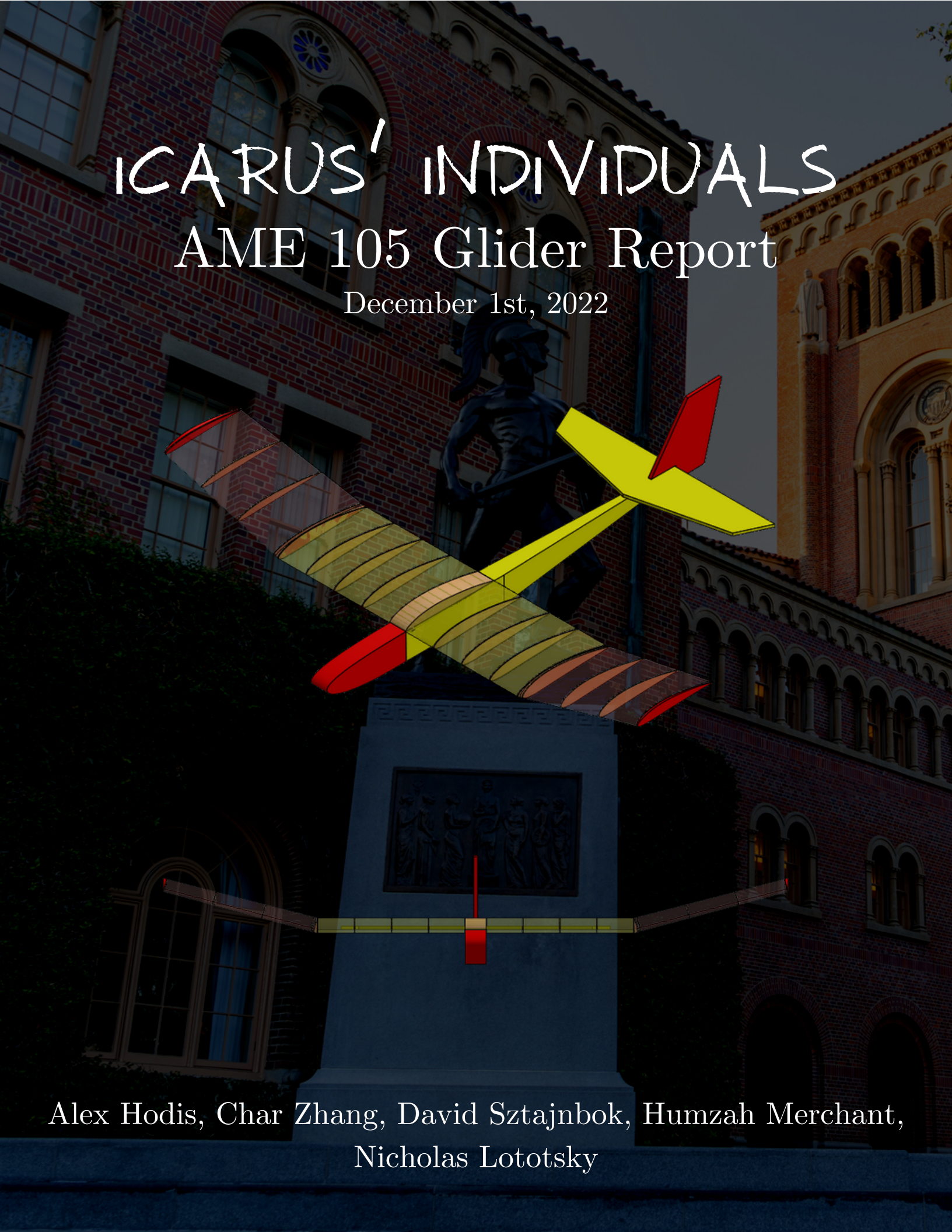

Alex Hodis, Char Zhang, David Sztajnbok, Humzah Merchant,
Nicholas Lototsky

Contents

Nomenclature

AR	Aspect Ratio
b	Wing Span
c	Wing Chord
D	Drag
e_v	Oswald Efficiency Factor
fus	Fuselage
h	Launcher Height
HS	Horizontal Stabilizer
K	Coefficient in $C_{D,i} = K{C_L}^2$
L	Lift
q	Dynamic Pressure $\frac{1}{2}\rho u^2$
R	Glider Range
Re	Reynolds Number
S	Planform Area
u	Flight Speed
VS	Vertical Stabilizer
W	Weight
α	Angle of Attack (AOA)
Δ	difference, Delta
γ	Glide Angle
μ	Dynamic Viscosity
ρ	Air Density
$\overline{X}$	Mean Value of X
c_d	Airfoil Profile Drag
C_f	Coefficient of Friction Drag
C_L	Coefficient of Lift
$C_{D,i}$	Induced Drag Coefficient
$C_{D,0}$	Zero-Lift Drag Coefficient of Glider
D_0	Zero-Lift Drag
D_f	Friction Drag
D_i	Induced Drag
Re_X	Reynolds Number of Component X
S_w	Wetted Surface Area
u_γ	Maximum Range Flight Speed

1 Introduction

1.1 Objectives

The main objective of this glider report is to compare the predicted and empirically determined flight performance metrics of the glider. Predictions were made using basic flight mechanics equations, assumptions, and measurements listed below. The empirical results were obtained by launching the glider from a catapult-like-apparatus, measuring its range and launch height, and evaluating the predictions with the same, fundamental equations.

1.2 Basic Equations of Flight Mechanics

In unaccelerated gliding flight, the three forces acting on a glider are given by fig(1): the force of gravity (W), lift (L), drag (D), and $\vec{u}$ is the velocity vector. Note that, by definition, $L \perp \vec{u}$ and $D \parallel \vec{u}$.

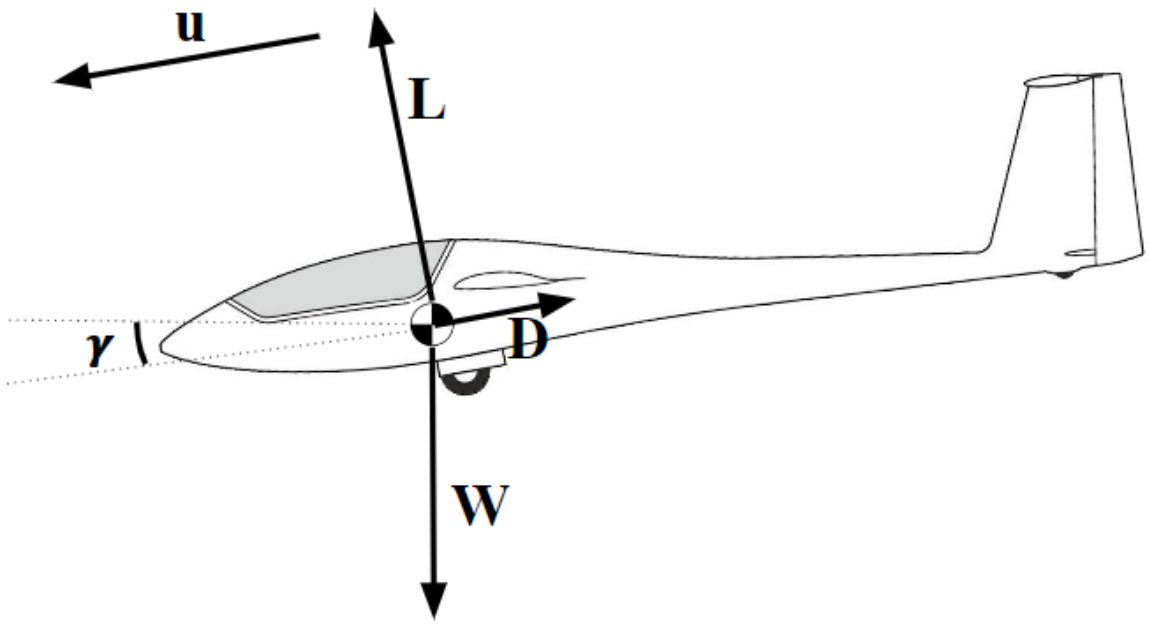

Figure 1: Free Body Diagram of a Glider in Steady Flight

Assuming that the glider descends at a constant angle γ, these three forces are related by

$$L = W \cos\gamma \tag{1}$$

and

$$D = W \sin\gamma \tag{2}$$

Dividing eq.(2) by eq.(1),

$$\frac{D}{L} = \tan\gamma. \tag{3}$$

Thus, from eq.(3), it is evident that γ is minimized when D/L is minimized, or equivalently, when L/D is maximized (commonly notated as $(L/D)_{max}$)). While the glider is not in level flight since $\gamma \neq 0$, to determine L, it is assumed $\gamma \approx 0$ such that $\cos\gamma \approx 1$. Thus, eq.(1) becomes

$$L = W \tag{4}$$

This simplification is useful since the weight of the glider remains constant throughout flight. Therefore, the necessary coefficient of lift, C_L, to maintain the relationship in eq.(4) can be determined for any flight speed u by

$$C_L = \frac{W}{\frac{1}{2}\rho u^2 S}, \tag{5}$$

where $\frac{1}{2}\rho u^2$ is the dynamic pressure (q) in terms of the atmospheric density, ρ, and the flight speed, u, and S is the planform area of the wings.

On the other hand, the total drag of the aircraft, D_{tot}, is given by

$$D_{tot} = D_0 + D_i \tag{6}$$

where the parasitic and induced components of the total drag are defined, respectively, as

$$D_0 = C_{D,0} q S_w \tag{7}$$

and

$$D_i = qSC_{D,i} \tag{8}$$

where $C_{D,0}$ is the parasitic drag coefficient, S_W is the wetted surface area, and $C_{D,i}$ is given by

$$C_{D,i} = K{C_L}^2. \tag{9}$$

K can be given in terms of the Oswald Efficiency, e_v, and the aspect ratio, AR, by the equation

$$K = \frac{1}{\pi e_v AR} \tag{10}$$

Combining eqs.(5-9), the total drag on the airplane as a function of flight speed is

$$D_{tot}(u) = \frac{1}{2} C_{D,0} \rho S u^2 + K \frac{W^2}{\frac{1}{2}\rho S u^2} \tag{11}$$

Thus, eq.(11) demonstrates that the parasitic component of drag varies proportionally to u^2 while the induced component of drag varies proportionally to u^{-2}.

Furthermore, another important value is the Reynolds Number (Re) given by

$$Re = \frac{\rho l u}{\mu} \tag{12}$$

where l is a characteristic length (mean chord, fuselage length, etc) and μ is the dynamic viscosity of the

fluid. Aerodynamic coefficients such as c_d are dependent on Re, with higher values of Re correlating to lower values of c_d.

1.3 Predictions

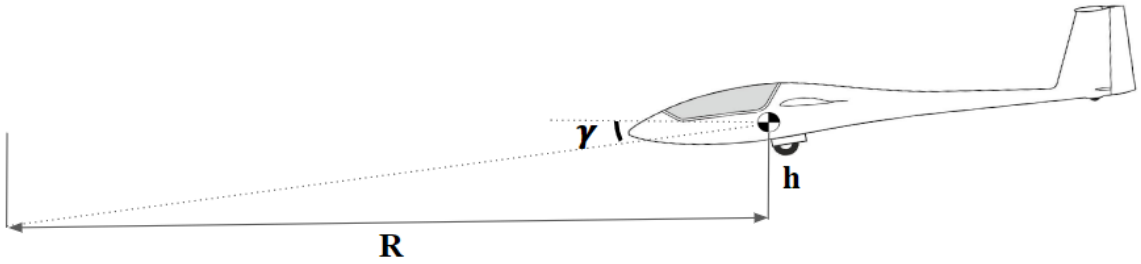

Figure 2: Range (R) and Launcher Height (h) Setup

Figure 2 shows that, assuming the glider maintain a constant γ throughout its flight, the flight range R and the launcher height h are related by

$$\tan\gamma = \frac{h}{R} \tag{13}$$

Combining eq.(3) and (13) gives

$$R = h(\frac{L}{D}). \tag{14}$$

Using eq.(4) and eq. (11), to calculate a function for the range as a function of flight speed, R(u), as

$$R(u) = h(\frac{W}{D_{tot}(u)}) \tag{15}$$

where $D_{tot}(u)$ is given by eq.(11). The maximum range is achieved at the speed u_γ, defined as the speed which minimizes the angle γ, and occurs at $D_{tot,min}$ (which is also $(L/D)_{max}$).
To make initial predictions of the glider's performance, the glider properties were estimated using values in Table 1.

Dimensions	Units	Value
Wing Span (b)	m	1.23
Wing Area (s)	m^2	0.27
Mean Chord ($\bar{c}$)	m	0.22
Aspect Ratio (AR)	-	5.59
Mass	kg	0.550
e_v	-	0.85
c_d	-	0.006
$C_{D,0}$	-	0.0103
h	m	2.0

Table 1: Predicted Parameters of the Glider

e_v was estimated based on a general expression found in Nita[2]:

$$e_v = \frac{1}{Q + P\pi A} \tag{16}$$

where Q and P are constants that describe the inviscid and viscous parts, respectively, of the induced drag. Using the constants from Obert[3] yields

$$e_v = \frac{1}{1.05 + 0.007\pi A} \tag{17}$$

which gives $e_v = 0.85$.

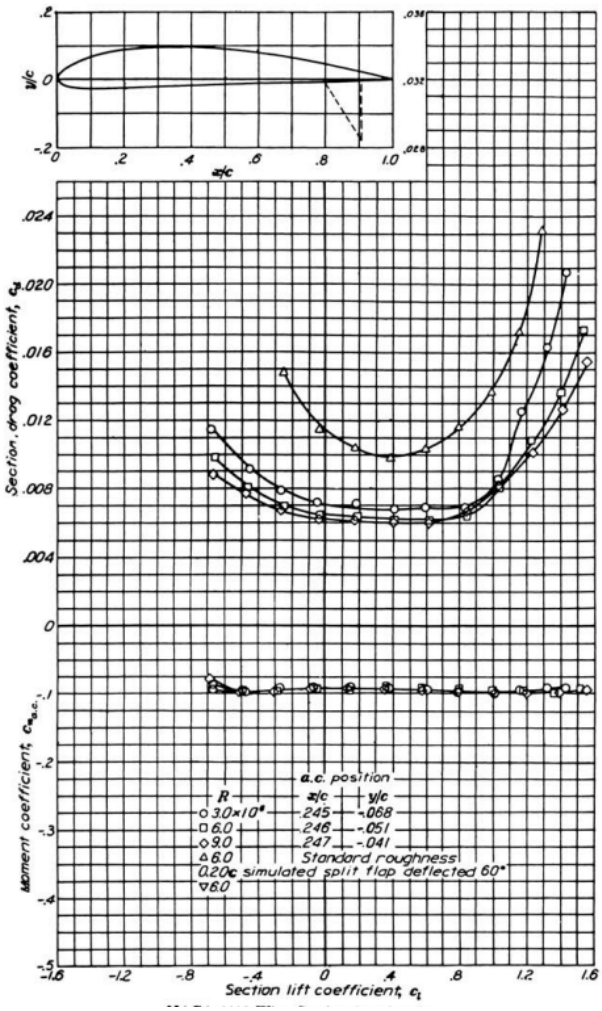

Figure 3: Drag Polar of a NACA 4412 Airfoil[1]

To estimate c_d, the Reynolds number was calculated using eq.(12) to be approximately 7.3×10^4 using $\nu = \dfrac{\mu}{\rho}$ as $1.5 \times 10^{-5}\text{m}^2/\text{s}$ under standard temperature and pressure, a nominal flight speed of $u = 5\text{m/s}$, and the mean chord length found in Table 1. c_d was predicted from the Figure 3 (see 2.1 for airfoil selection), using the lowest Reynolds Number in the figure of 3.0×10^6, which, despite being about 2 orders of magnitude greater than the predicted Re, was the closest Re value. The profile drag of the airfoil and the friction drag of the entire airplane (see 3.1 for calculations) were used to predict $C_{D,0} = 0.0103$ for the glider.

With these measured and the predicted values, the total drag of the airplane and its parasitic and induced components were calculated using eq.(6), (7), and (8), and the resulting values for drag as functions of flight speed are shown in Figure 4.

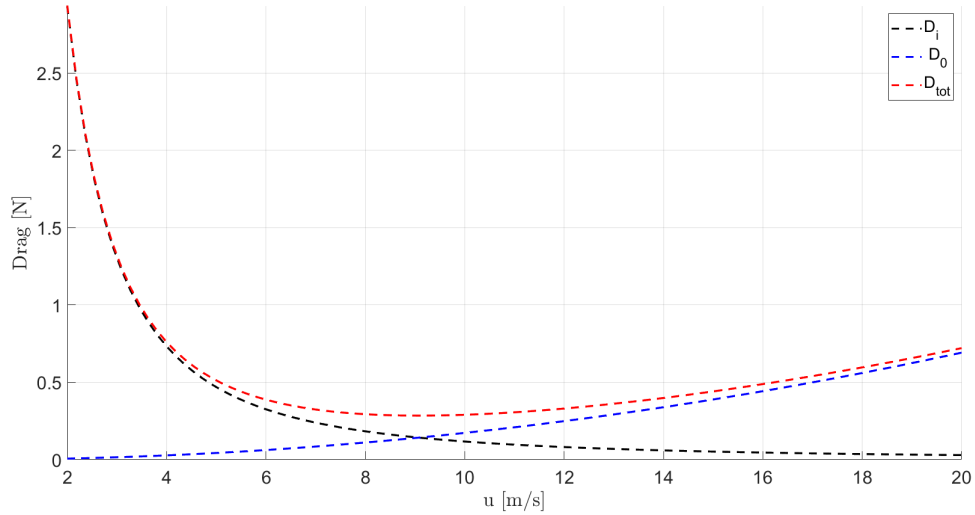

Figure 4: Drag as a Function of Flight Speed

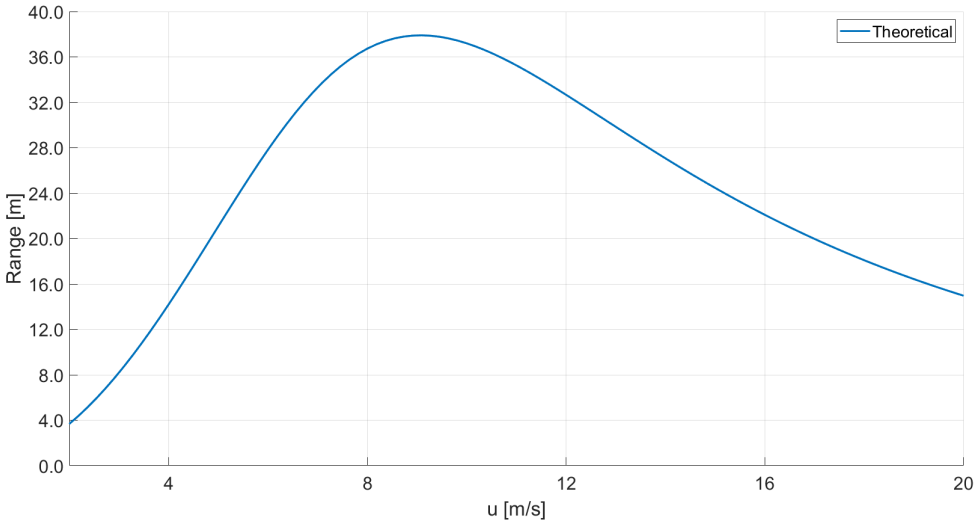

Figure 5: Range as a Function of Flight Speed

With $D_{tot}(u)$ predicted, eq.(15) was used to create a prediction for the flight range as a function of flight speed shown in Figure 5. The best range speed, u_γ, was predicted to be 9.0m/s with an $(L/D)_{max}$ of 19.0 and a range of approximately 38.0m. To compare actual and theoretical data, the range as a function of launch height and launch speed must be measured.

2 Materials and Methods

2.1 Glider

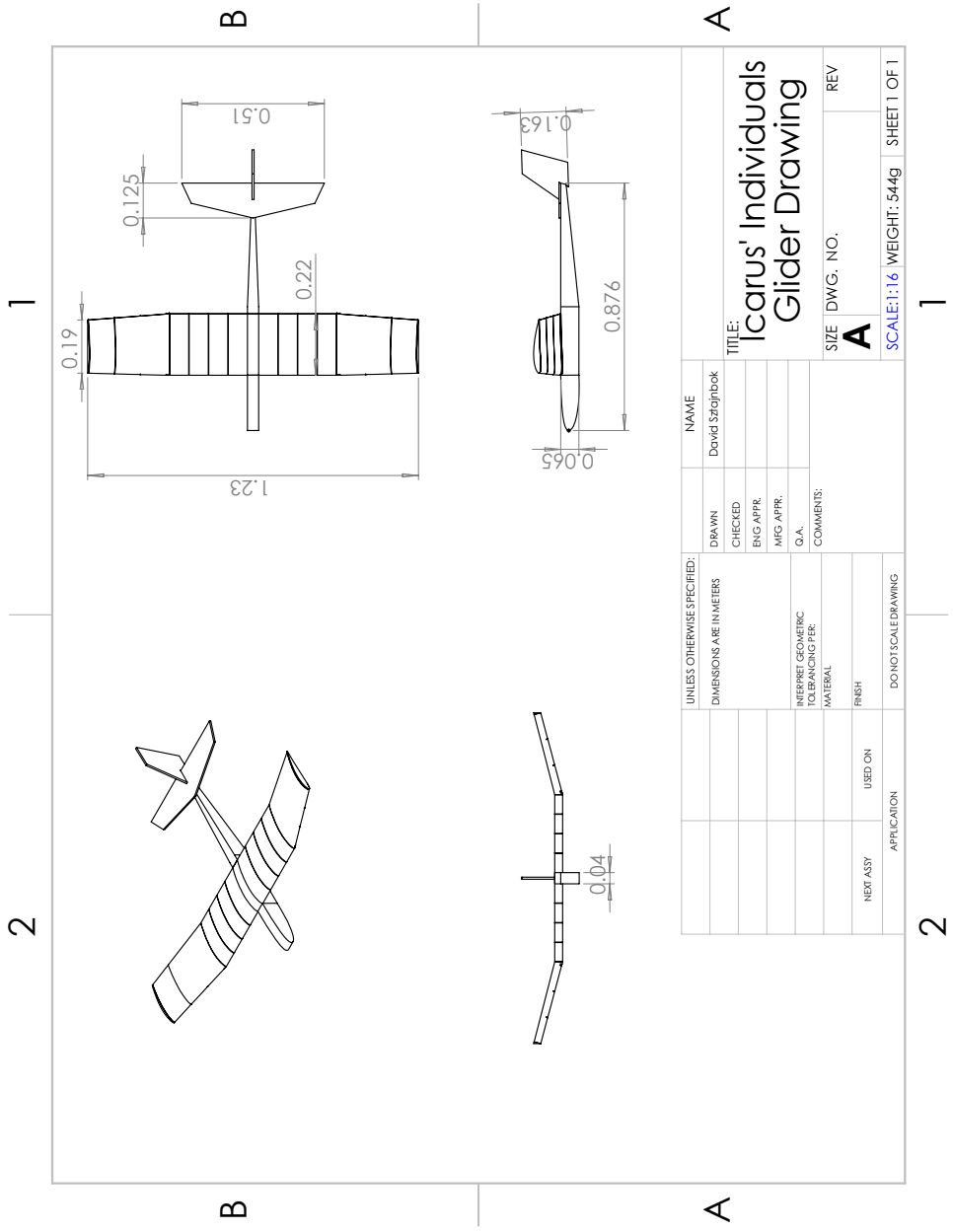

Figure 6: Dimensioned Multiview of the Glider

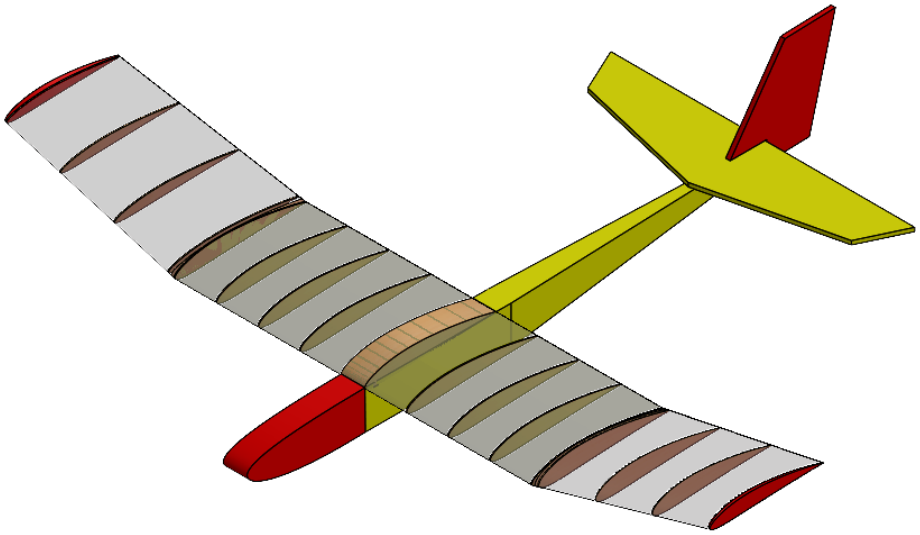

Figure 7: 3D Model of the Glider

Table 2: Basic Geometries and Measurements

Dimensions	Units	Value
Wing Span (b)	m	1.23
Wing Area (s)	m^2	0.27
Mean Chord ($\bar{c}$)	m	0.22
Aspect Ratio (AR)		5.59
Mass	kg	0.554

Table 3: Airfoil Parameters (measured on Root Chord)

Dimensions	Units	Value	Percent Chord (%)
Maximum Chamber	cm	1.0	4.4
Position Maximum Chamber	cm	8.1	35
Maximum Thickness (t)	cm	2.8	12

The glider had a uniform airfoil profile throughout its span, so measurements of the chamber and thickness were taken along the root chord and normalized by the root chord length. The nearest resulting NACA airfoil is a NACA 4412. The glider's airfoil had a flat bottom, while the NACA 4412 has a slightly curved bottom, though the airfoils are very similar across other parameters and therefore no major differences in performance were predicted.

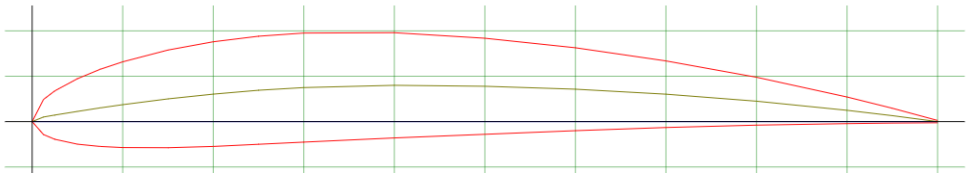

Figure 8: NACA 4412 Airfoil

2.2 Testing Procedures

The purpose of the tests was the measure the flight range of the glider at a variety of known launch speeds and from a known height. The electrically-powered launcher accelerated the glider over an approximately 3 meter long distance from a height of 1.75 meters. Flight tests were conducted in the early morning to minimize wind, and the temperature and pressure were recorded from the USC weather station. Before each flight, the plane's weight W was measured. A target launch speed was set for each flight and the glider's actual launch speed u was recorded. The flight duration s was measured with a timer and the lateral position xft and horizontal distance yft locations of where the glider first touched the ground were recorded. The range of the glider was calculated using the Pythagorean theorem,

$$x^2 + y^2 = R^2$$

where R is the total range. This model simplifies the actual flight path of the glider (which takes a more curved trajectory) and results in underestimating the range.

Table 4: Test Flight Conditions

Condition	Start (x_0)	End (x_1)	Average ($\overline{x}$)	$\Delta x/\overline{x}$
Launch Rail Height [m]	1.75	1.75	1.75	0%
Temperature [K]	282	286	284	0.7%
Pressure [Pa]	1.03×10^5	1.03×10^5	1.03×10^5	0%

3 Results

3.1 Reynold's Number and Drag Estimates

Eq.(12) was used to calculate the Reynold's number, with the results listed in Table 4 for each component. Assuming $Re_{cr} = 5 \times 10^5$, and $Re_{fus} < Re_{cr}$, $Re_{vs} < Re_{cr}$, and $Re_{hs} < Re_{cr}$, therefore laminar flow can also be assumed. Thus, the coefficient of friction drag for each component can be calculated by

$$C_f = \frac{1.328}{\sqrt{Re_l}}. \tag{18}$$

the friction drag for each component can then be determined by

$$D_f(u) = qS_wC_f. \tag{19}$$

The density during the flight tests was calculated by

$$\rho = \frac{p}{RT} \tag{20}$$

where p is the atmospheric pressure, R is the specific gas constant, and T is the absolute temperature. This yielded a density of 1.26kg/m^3. The kinematic viscosity, ν, is defined as

$$\nu = \frac{\mu}{\rho} \tag{21}$$

and is $1.5\times10^{-5}\text{m}^2/\text{s}$ at standard temperature and pressure conditions. Since standard density is $1.23\text{kg}/\text{m}^3$, ν was adjusted for nonstandard density by dividing by $\frac{1.26}{1.23}$, yielding a value of $1.45\times10^{-5}\text{m}^2/\text{s}$. Using eq.(12) and an average flight speed of 8.9m/s, the Re and friction drag for each component is listed Table 5.

Table 5: Re calculations

Component	Length [m]	S_w [m^2]	Re	C_f	D_f[N]
Fuselage	0.876	0.127	$5.03\times10^5\pm.7\%$	1.87×10^{-3}	0.0119
Horizontal Stabilizer	0.105	0.0928	$6.03\times10^4\pm.7\%$	5.38×10^{-3}	0.0250
Vertical Stabilizer	0.120	0.0329	$6.89\times10^4\pm.7\%$	5.06×10^{-3}	8.31×10^{-3}
Total	-	-	-	-	0.045

3.2 Range vs. Flight Speed

Table 6: Flight Test Data

Flight	$U_0[m/s]$	Duration [s]	x [m]	y [m]	Range (R) [m]	mass (g)	Remarks
1	5	2.2	-1.8	7.6	7.8	554	Left Roll
2	7	1.7	-0.3	12.5	12.5	554	
3	9.1	3.1	-1.8	18.9	19.0	554	+2 degrees α_i, pitch up
4	10.4	2.1	-2.1	16.5	16.6	554	Shims removed
5	8.8	2.6	0.3	19.5	19.5	554	Added more right trim
6	9.1	3.0	0.6	21.9	21.9	554	Straight flight
7	10.4	1.9	-1.5	14.6	14.7	554	Pitched down
8	8.5	2.5	-2.1	15.2	15.4	554	Left, up elevator trim
9	8.4	2.6	0.3	18.6	18.6	554	Straight, up elevator
10	8.9	3.3	-4.0	20.1	20.5	554	pitched up
11	10.1	2.8	-0.3	20.4	20.4	554	$+1\alpha_i$
12	11.1	1.4	-1.2	14.9	15.0	554	-2α_i, lifted early
Average	8.9	2.4	-1.2	16.7	16.8	554	
S.D.	-	0.59	1.3	4.0	4.18	0	

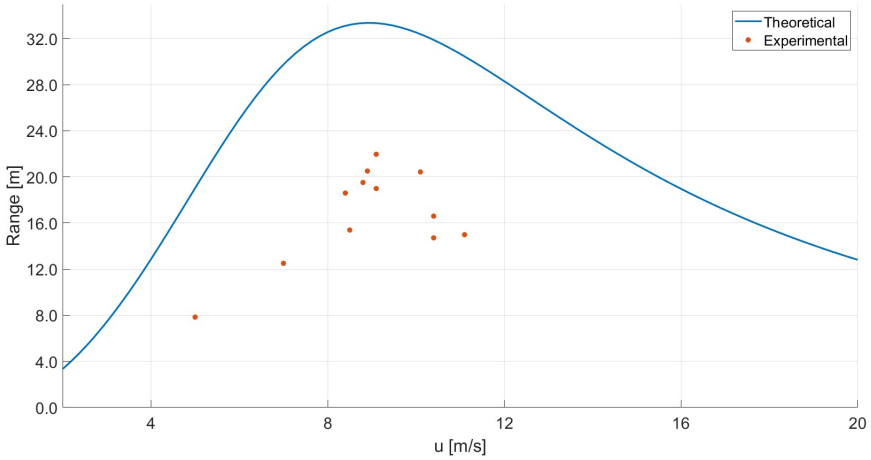

Figure 9: Theoretical and Experimental Range vs. Flight Speed

Figure 9 demonstrates that for every experimental flight speed, the theoretical range (adjusted for new measured launch conditions) predicted the glider would travel further, with a consistent underperformance of about $30-50\%$. The under-performance was more significant at extreme speeds, both high and low (relative to u_γ), likely because the AOA was not adequately adjusted between every flight (see Table 6 for flights where AOA was adjusted). The experimental data does follow the same distribution as the theoretical data, however.

Table 7: Average Duration and Range by Flight Speed with 1 S.D. Interval

Speed Range [m/s]	Number of Flights	Average Duration [s]	$\overline{\lvert x \rvert}$ [m]	$\overline{y}$ [m]	$\overline{R}$ [m]
$U < 8$	2	2.0 ± 0.35	1.1 ± 1.1	10.1 ± 3.45	10.2 ± 3.3
$8 \leq U < 9$	4	2.8 ± 0.37	1.68 ± 1.8	18.4 ± 2.17	18.5 ± 2.2
$9 \leq U < 10$	2	3.1 ± 0.071	1.28 ± 0.78	20.4 ± 2.16	20.5 ± 2.1
$U > 10$	4	2.1 ± 0.58	1.41 ± 0.7	16.9 ± 2.7	17.0 ± 2.6

Table 7 demonstrates that flights with a launch velocity between 9m/s and 10m/s had the longest duration (with an average of 3.1s) and range (with an average of 20.5m). Notably, flights in this speed range were also some of the straightest, with an average horizontal offset of 1.28m. Since values of x could be both negative of positive, the average of the absolute value was taken, so this average represents the average magnitude of lateral displacement.

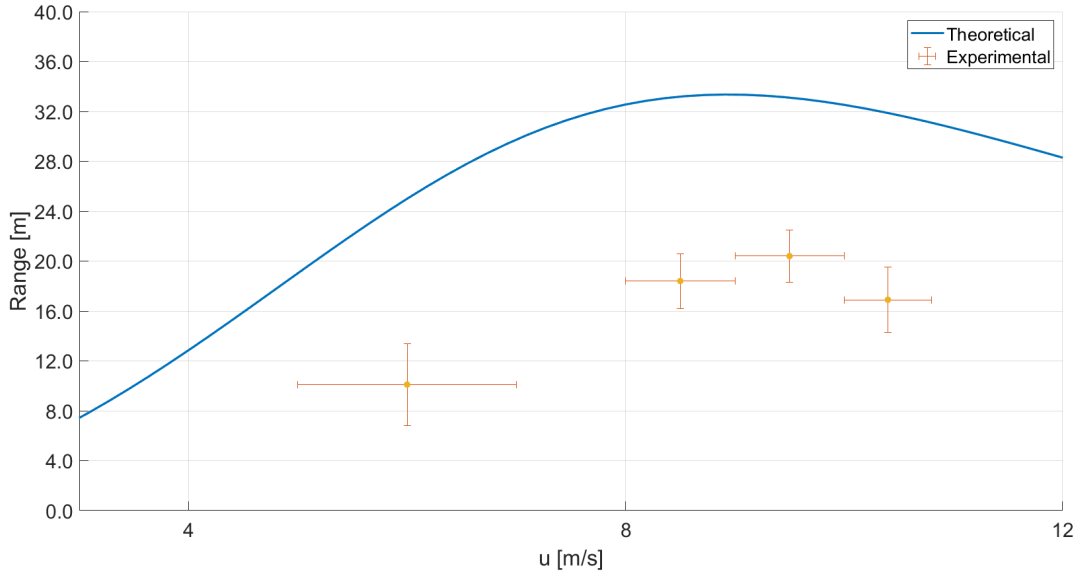

Figure 10: Theoretical and Experimental Range with Standard Deviation as a Function of Flight Speed

The average ranges ($\overline{R}$) and their associated standard deviations are plotted and compared against the theoretical range. This demonstrates that there was a statistically significant difference between the measured ranges of gliders and the predicted range. There is more variation for range at speeds other than u_γ, likely because the AOA was adjusted for only some flights, and thus the C_L for $(L/D)_{max}$ was not achieved for every flight. However, since no flight exhibited abnormal behavior such as excessive floating in ground effect or apparent climbing/descending other than a constant descent path, all flights were used for data analysis.

4 Discussion

4.1 Theory and Experiment Comparison

The glider under-performed by approximately 30% compared to the theoretical range. The overall distribution of actual ranges matches the predicted distribution and the best range flight speed (u_γ) of about 9.1m/s matched the predictions. The most likely reasons for the difference between theory and experiment are the e_v and $C_{D,0}$ values used for the predictions as other variables were measured with less uncertainty.

From eq.(5), the flight speed u can be written as a function of C_L as

$$u = \sqrt{\frac{2W}{\rho S C_L}} \tag{22}$$

At u_γ, $C_{D,0} = C_{D,i}$. Combining with eq.(10),

$$C_L = \sqrt{\frac{C_{D,0}}{K}} \tag{23}$$

Thus,

$$u_\gamma = \sqrt{\frac{2W}{\rho S}\sqrt{\frac{K}{C_{D,0}}}} = \sqrt{\frac{2W}{\rho S}\sqrt{\frac{1}{(\pi e_v AR) C_{D,0}}}} \tag{24}$$

.

From eq.(24), it is evident that $u_\gamma \propto (\frac{1}{C_{D,0}})^{0.25}$. Furthermore, from eq.(25), $(L/D)_{max}$, and thus range, is proportional to $\frac{1}{\sqrt{C_{D,0}}}$. This is corroborated by Figure 11, where increasing values of $C_{D,0}$ show decreasing maximum range and a decreasing u_γ.

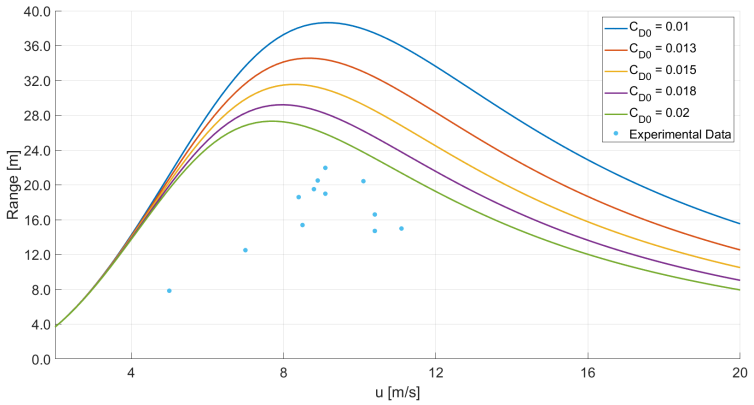

Figure 11: Range as a Function of Flight Speed with Varying $C_{D,0}$

Eq.(24) also demonstrates that $u_\gamma \propto (\frac{1}{e_v})^{0.25}$. Since $e_v < 1$, decreasing values of e_v results in higher u_γ. Additionally, eq.(25) demonstrates that $R \propto \frac{1}{\sqrt{K}} \propto \sqrt{e_v}$. Thus, higher values of e_v result in a higher range (very expected). This is corroborated by Figure 12, where the range decreases with lower e_v but u_γ increases.

Since the glider had a u_γ comparable to predicted value but a range of a much smaller magnitude, the

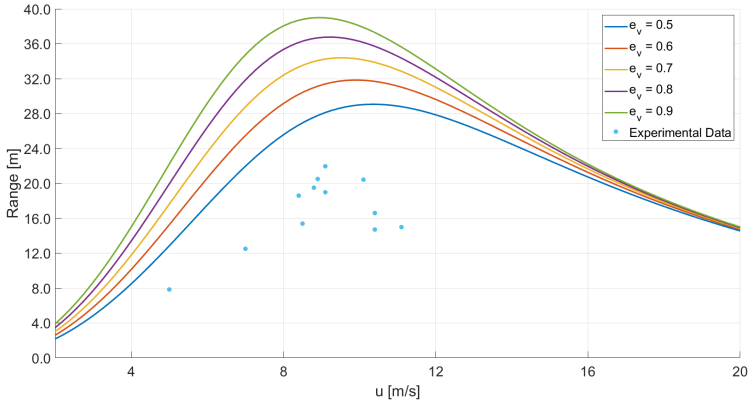

Figure 12: Range as a Function of Flight Speed with Varying e_v

value of $C_{D,0}$ was likely too low but e_v was overestimated; notably, however, the ratio $\frac{K}{C_{D,0}}$ was correct as this ratio determine u_γ (refer to Section 4.4).

4.2 W/S

Using $W = mg$, the weight is found to be $W = 5.43N$. With $S = 0.27m^2$, this yields a value for wing loading:

$$\frac{W}{S} = 20.1\frac{\text{kg}}{\text{m}^2}$$

Wing loading can be examined as dependant on two primary values: weight (a measure of scale, or size) and speed. Heavier aircraft, all else being equal, require a higher wing loading since more weight must be supported by the same amount of lifting surface. Faster aircraft also have higher wing loading sine more aerodynamic load is exerted on the lifting surface (heaving aircraft have to fly faster since $u \propto \sqrt{l}$. A plot of the wing loading of various planes and birds (taken from [4]) versus weight in a logarithmic scale is shown below:

The glider falls on the trend line. Note that its wing loading is slightly lower, though. This can be explained

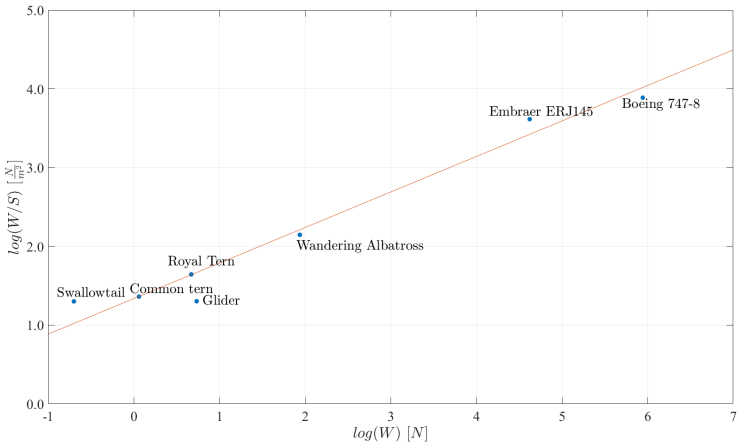

Figure 13: Wing Loading versus Weight in a logarithmic scale for various flying objects and animals.

by the glider's small weight, especially considering it was designed to have a gas engine, servos, etc., all of which were replaced with CG-adjusting clay.

4.3 $(L/D)_{max}$

4.3.1 Derivation of $(L/D)_{max}$ in terms of K and C_{D_o}

$(L/D)_{max}$ can be written in terms of K and C_{D_o}. From eq.(12), it is possible to find that, at $(L/D)_{max}$, the following is true

$$C_{D_o} = K{C_L}^2$$

C_L can thus be written as

$$C_L = \sqrt{\frac{C_{D_o}}{K}}$$

Also, note that

$$(\frac{L}{D})_{max} = (\frac{C_L}{C_{D_{tot}}})_{max}$$

It then follows that

$$(\frac{C_L}{C_{D_{tot}}})_{max} = \frac{C_L}{C_{D_o} + K{C_L}^2} = \frac{\sqrt{\frac{C_{D_o}}{K}}}{C_{D_o} + K\frac{C_{D_o}}{K}} = \frac{\sqrt{\frac{C_{D_o}}{K}}}{2C_{D_o}}$$

Rewriting the expression above gives an interesting expression for $(L/D)_{max}$:

$$(\frac{L}{D})_{max} = \frac{1}{2\sqrt{KC_{D_o}}} \tag{25}$$

4.3.2 Comparisons

Using eq.(15) and the values in Table 6, the empirical $(L/D)_{max}$ is

$$(\frac{L}{D})_{max,empirical} = 12.5$$

Using eq.(24), the theoretical $(L/D)_{max}$ is

$$(\frac{L}{D})_{max,theoretical} = 19.0$$

The difference can be explained primarily by drag and range predictions. An underestimation of C_{D_o} (see Appendix) and an overestimation of range lead to a much higher predicted $\frac{L}{D}$.

4.4 U_γ

U_γ is the flight speed that minimizes the glide angle. It can be predicted using the relationship

$$U_\gamma = \sqrt{\frac{2W}{\rho S C_L}} = \sqrt{\frac{2W}{\rho S} \cdot \sqrt{\frac{K}{C_{D,0}}}}.$$

K can be calculated using eq.(11) and values from Table 1 and 2, resulting in $u_\gamma = 9.1$m/s. During the experiment, the output velocity of the launch varied, and the maximum range of 21.9m was achieved at

$u = 9.1$m/s. There is a key limitation in using 9.1m/s as u_γ as no other flight speeds between 9 and 10 m/s were recorded, but the two flights at 9.1m/s had the highest average range of any speed range (Table 7). This means that the predicted u_γ equals the measured u_γ.

4.5 C_L

Assuming steady level flight at U_γ

$$C_L = \frac{W}{qS} = 0.4$$

The set AOA of the glider (angle of incidence) is $2.5 \pm 1deg$. Using

$$C_L = (c_{l\alpha}\frac{AR}{AR+2})(\alpha - \alpha_{0L}), \tag{26}$$

where $c_{l\alpha}$ is the slope of the $c_l v.\alpha$ plot for the airfoil and α_{0L} is the AOA at which the airfoil has $c_l = 0$. Using Figure 9 and assuming Re $= 3.0 \times 10^6$, $c_{l\alpha} = 0.10$ / deg and $\alpha_{0L} = -4$ deg. Thus, $C_L = 0.48$.

The actual C_L was 17% lower than predicted, which is why shims were used to lower the AOA on some flights, especially higher-speed flights.

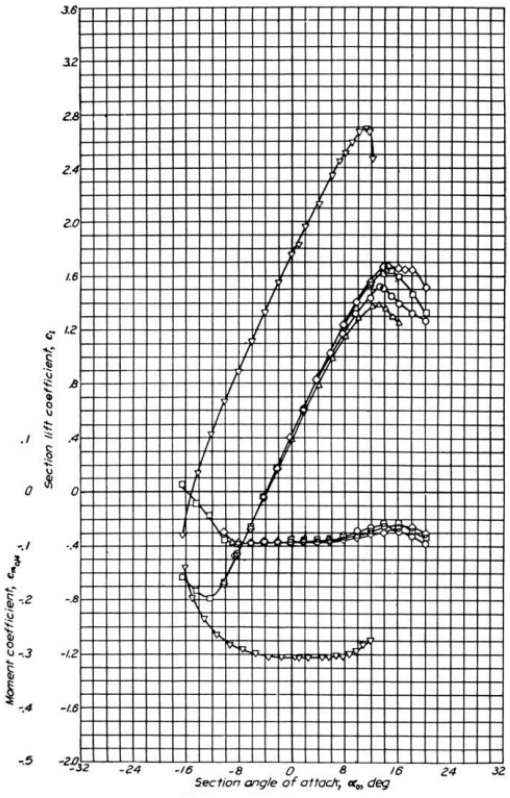

Figure 14: C_L as a Function of α for a NACA 4412 Airfoil [1]

5 Summary

The glider did not perform as predicted. Although u_γ was the same for both theory and experiment, around 9m/s, the actual distance the glider flew was more than a standard deviation less than the predicted distance. Theory predicted that the glider would fly around 33 meters when travelling at 9m/s, while in the experiment it only travelled 21 meters at the same speed. At every speed the glider was tested at, the experimental distance was about 30% less than the predicted theoretical distance. It is probable that e_v was estimated too high and the $C_{D,0}$ was estimated too low since a perfectly smooth body at higher than actual Reynolds numbers was assumed in the theoretical calculations. However, since u_γ was predicted well, an accurate ratio of K to $C_{D,0}$ was determined, though the values of K and $C_{D,0}$ can be varied for a more accurate characterization of flight range (see Appendix).

6 References

[1] J.D. Anderson. *Introduction to Flight.* Aeronautical and Aerospace Engineering Series. McGraw-Hill, 1985.

[2] M. Niţă and D. Scholz. *Estimating the Oswald Factor from Basic Aircraft Geometrical Parameters.* Deutsche Gesellschaft für Luft- und Raumfahrt - Lilienthal-Oberth e.V., 2012.

[3] E. Obert, R. Slingerland, D.J.W. Leusink, T. van den Berg, J.H. Koning, M.J.L. van Tooren, and Technische Hogeschool Delft. Afdeling der Luchtvaart-en Ruimtevaarttechniek. *Aerodynamic Design of Transport Aircraft.* Ios Press, 2009.

[4] H. Tennekes. *The Simple Science of Flight, revised and expanded edition: From Insects to Jumbo Jets.* Mit Press. MIT Press, 2009.

Division of Labor

Nicholas worked on the graphs, section 1, and 3.2. David worked on the CAD model and drawings, section 4.2, section 4.3, and cover. Alex worked on section 2, section 3, section 4.1, and section 5. Char worked on sections 4.4 and 4.5. Humzah worked on sections 2.2, 4.2 writeup and graph, 4.5, and 5. Though these are some specific designations/assignments, everyone reviewed each others' work and many parts were, in practice, the work of many or even all.

Appendix: Optimization of Oswald Efficiency and $C_{D,0}$

Table 8: Flight Test Data used for Optimization

Flight	$U_0[m/s]$	Duration [s]	x [m]	y [m]	Range (R) [m]	mass (g)	Remarks
2	7	1.7	-0.3	12.5	12.5	554	
5	8.8	2.6	0.3	19.5	19.5	554	Added more right trim
6	9.1	3.0	0.6	21.9	21.9	554	Straight flight
9	8.4	2.6	0.3	18.6	18.6	554	Straight, up elevator
10	8.9	3.3	-4.0	20.1	20.5	554	pitched up
11	10.1	2.8	-0.3	20.4	20.4	554	$+1\alpha_i$

In order to reduce the uncertainty of the range prediction model given by eq.(15), a sweep optimization was performed to optimize the e_v and $C_{D,0}$. For this analysis, flights with a range of speeds were selected, but flights with the maximum range for each speed range were selected as their would yield an optimization with less uncertainty. The Oswald Efficiency was varied from 0.3 to 1 and $C_{D,0}$ was varied from 0.001 and 0.03. For each pair of values, an equation for $R(u)$ was generated from eq.(15). Then, for each flight listed in Table 8, the theoretical range using that pair of e_v and $C_{D,0}$ was calculated, and a weighted difference using

$$d_{i,j} = 1/\sum_{k=1}^{6}(R_{i,j}(u_k) - u_k)^2 \tag{27}$$

where $d_{i,j}$ represents the inverse relative total difference between the model using the ith value of e_v and the jth value of $C_{D,0}$ and the actual flight data, $R_{i,j}$ represents the theoretical range for the pair of values, and u_k is the kth test flight speed. To ensure that the optimized model maintains a similar u_γ, $d_{i,j}$ for pairs of values that results in a $u_\gamma < 9$ or $u_\gamma > 10$ were removed. The optimized (i, j) pair were found by finding the indexes of

$$max(d_{i,j}). \tag{28}$$

This yielded $e_v = 0.657$ and $C_{D,0} = 0.0182$. Figure 14 shows the optimized range plotted against experimental data, showing that the prediction is a better representation of the ideal performance of the glider. There is still $20 - 30\%$ difference between some actual ranges and theoretical ranges. This is most prevalent at speeds other than u_γ because the glider's AOA was not properly adjust for each flight to achieve the desired C_L. Thus, the glider was not flying at $(L/D)_{max}$ for those flights.

Using eq.(25) with the optimized values yields 12.6, just a 0.8% difference between the measured $(L/D)_{max}$ of 12.5. While there is still uncertainty in these predicted values, this optimization provides a foundation to base future estimates of this glider's range.

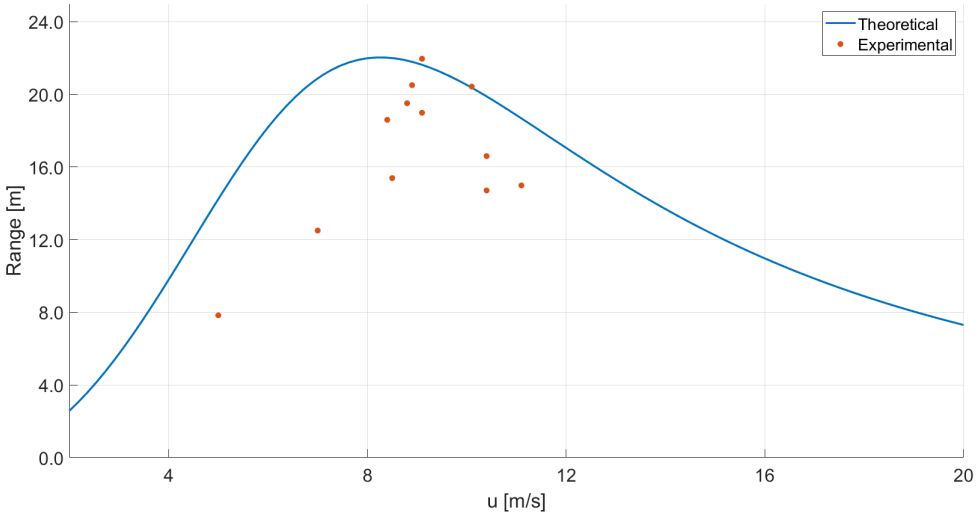

Figure 15: Optimized Theoretical and Actual Range as a Function of Flight Speed

Conflicts of Interest

The authors of this paper declare that they have no conflicts of interest or other competing financial interests.